

New disease outbreak affects two dominant sea urchin species associated with Australian temperate reefs

Michael Sweet^{1,*}, Mark Bulling¹, Jane E. Williamson^{2,3}

¹Molecular Health and Disease Laboratory, Environmental Sustainability Research Centre, College of Life and Natural Sciences, University of Derby, DE22 1GB, UK

²Department of Biological Sciences, Macquarie University, Sydney, New South Wales 2109, Australia

³Sydney Institute of Marine Science, Mosman, New South Wales 2088, Australia

ABSTRACT: Diseases of sea urchins have been implicated in dramatic transitions of marine ecosystems. Although no definitive causal agent has been found for many of these outbreaks, most are hypothesised to be waterborne and bacterial. Here we show the first report of a novel disease affecting at least 2 species of urchins off the south-eastern coast of Australia. The aetiological agent, identified via a range of molecular techniques, immuno-histology and inoculation experiments, was found to be the opportunistic pathogen *Vibrio anguillarum*. The disease appears to be temperature-dependent, with a faster transmission rate and increase in prevalence during experimental trials conducted at higher temperatures. Furthermore, analysis of long-term field data suggests that it may have already reached epidemic proportions. With the increases in ocean temperatures brought about by climate change, this novel urchin disease may pose a severe problem for the organisms associated with the temperate reefs off Australia and/or the ecosystem as a whole.

KEY WORDS: *Holopneustes purpurascens* · *Heliocidaris erythrogramma* · Pathogen · *Vibrio* · Henle-Koch postulates · Echinoderm

Resale or republication not permitted without written consent of the publisher

INTRODUCTION

Occurrences of diseases are reported to be increasing worldwide and, for a diversity of taxa, large-scale outbreaks of disease have been associated with climate change and other anthropogenic stresses (Harvell et al. 1999, Campbell et al. 2014). In particular, profound and rapid changes are occurring at global and regional scales within marine environments. Mean sea temperature has risen by 0.2°C decade⁻¹ (Pachauri et al. 2014) and oceanic pH has decreased, on average, from 8.2 to 8.1 since the industrial revolution (Zeebe 2012). It is hypothesised that these changes are stressing marine organisms, causing range shifts in distribution in many taxa and

leading to increasing susceptibility of these organisms to opportunistic pathogens (Ainsworth et al. 2010, Campbell et al. 2014). Echinoids, in particular, have experienced substantial declines associated with disease in the past half century (Feehan & Scheibling 2014). Urchins are often key components of marine communities (Sammarco 1982, Scheibling & Hennigar 1997), limiting algal biomass by extensive grazing and being an important food source for many predators. The result of the balance between algal and urchin biomass can range from kelp forests to urchin-dominated 'barrens'. However, transitions can occur between these states as a result of factors associated with climate change that result in changes to nutrient supply, the number and type of predators,

*Corresponding author: m.sweet@derby.ac.uk

variation in the frequency and intensities of storms and increases in incidence of diseases, for example (Sammarco 1982, Steinberg 1995, Scheibling & Hennigar 1997).

In some instances, urchin diseases are necessary to regulate populations in the absence of natural predators such as many fish species, a result brought about by overfishing around the world (Lafferty 2004). However, disease outbreaks can also have large impacts on urchin populations and the ecosystems they inhabit. In 1983, for example, the dominant urchin of Caribbean coral reefs, *Diadema antillarum*, experienced massive disease-induced mortality, and the functional effects of this decline continue to persist today (Mumby et al. 2006). Prior to the decline, *D. antillarum* could be found in densities exceeding 70 m^{-2} (Sammarco 1982) and was considered to be one of the most important grazers on Caribbean reefs (Carpenter 1986, Mumby et al. 2006). It is now widely agreed that its loss across much of its range led to a dramatic decline in coral cover throughout the Caribbean (Sammarco 1982, Mumby et al. 2006), and the decline of this urchin is still considered to be the greatest recorded mass mortality of a marine animal, with functional recovery remaining unlikely more than 30 yr on (Levitán et al. 2014).

On the other side of the world, Australia is a well-known diversity hotspot for sea urchin species (Miskelly 2002), in particular the temperate waters off the south-eastern coast. Two of the more abundant species in these ecosystems are *Heliocidaris erythrogramma* (Valenciennes, 1846) and *Holopneustes purpurascens* (Agassiz, 1872). Both species inhabit shallow subtidal kelp habitats but have different life history characteristics in the manner that they use the habitat. *H. erythrogramma* commonly occurs on the substratum, consuming a range of foliose and crustose algae (Wright et al. 2005), whereas *H. purpurascens* lives largely enmeshed in the canopy of the algae it consumes, using the algae as a habitat in addition to a food source, thus limiting its distribution because of its restricted diet breadth (Williamson et al. 2004). Both species have the capacity to substantially impact the demography and diversity of other flora and fauna in these habitats (Pederson & Johnson 2007, Bell et al. 2014). During regular surveys conducted in this region in 1996, a previously unreported disease was noted. The disease was first recorded after unusually high-density aggregations of *H. erythrogramma* occurred in the previous year (1995), and these high densities continued for a further 3 yr (Wright et al. 2000). In this study, we document the long-term prevalence of the disease, assess

the modes of transmission, aim to identify the pathogen(s) responsible and assess the influence of temperature on transmission and spread, which is in itself a well-documented abiotic factor that is increasing at approximately 4 times the global average within the region (Ridgway 2007).

MATERIALS AND METHODS

Long-term monitoring and current prevalence of lesions

Trends in the prevalence of lesions in *Holopneustes purpurascens* were assessed using long-term monitoring records, which were collected from 1996 to 2013. Populations associated with the shallow rocky reef habitat near Bare Island off the coast of Sydney, Australia ($151^{\circ} 13' 52'' \text{E}$, $33^{\circ} 59' 32'' \text{S}$), were measured, taking into account the size of the individual (diameter), sex of the individual and the number of lesions present. During sampling, random individuals were collected from the population. This was because *H. purpurascens* wrap themselves within the canopy of the algae they inhabit (Steinberg 1995), any lesions on individuals were therefore not always obvious at the time of collection *in situ*. Such random sampling enables unbiased assessment of the numbers of diseased vs. healthy individuals. Animals were collected at various times throughout each year, usually in groups of 10 or 20. However, the extent of sampling from year to year was inconsistent (minimum = 14, maximum = 540, median = 111) and sampling did not occur in some years (1999, 2000, 2002, 2007, 2011). To account for this heterogeneity and to ensure robust analysis, only records from years when >99 individuals were collected were included in the long-term analysis. In addition, we also wanted to assess whether disease abundance varied between sexes. *H. purpurascens* is usually gonochoristic, with a sex ratio of 1:1 (Williamson & Steinberg 2002), and this was found in our sampling ($\chi^2 = 0.99$, $\text{df} = 1$, $p = 0.32$). To assess whether there was a sex bias in the presence of lesions, a chi-squared goodness-of-fit test was conducted on pooled (years) survey results. Relationships between size (diameter), sex and presence of lesions were also assessed in a similar way, using logistic regression. Males and females appeared to be equally affected by lesions over the 17 yr of sampling ($\chi^2 = 0.88$, $\text{df} = 1$, $p = 0.35$), and there was no significant relationship between the size of the individual and the occurrence of lesions over time (Hosmer-Lemeshow = 3.70, $\text{df} = 8$, $p = 0.88$).

Identification of potential aetiological agents

During 2012 and 2013, tissue samples from *H. purpurascens* and *Heliocidaris erythrogramma* were taken for microbial and histological analysis to describe the pathogenesis of the characteristic dark lesions (see Fig. 1) which were first observed to affect the wild populations in 1996. The aim of this part of the study was to identify any potential causal agents associated with the disease. Sterile swabs were used to collect surface-associated microbiota *in situ* from live animals, whilst a different subset of animals were collected whole from the field. Both sample types were then stored in 100% ethanol until extraction and further analysis. Healthy (n = 20) and diseased (n = 20) individuals from both species were collected from 2 locations where the disease was prevalent: Bare Island in Botany Bay and Fairlight in Port Jackson (151° 16' 32" E, 33° 48' 1" S). For microbial and histological analysis, samples were separated into healthy tissue (n = 20 from individuals that were free of lesions), apparently healthy tissue (n = 20 from individuals with lesions present, adjacent to the lesion interface) and n = 20 of the tissue directly associated with the lesions. Tissues from these whole animals were subsequently removed under sterile conditions and crushed using a mortar and pestle. A further set of n = 20 urchins (n = 10 each, healthy and diseased) from each species were dissected and the coelomic fluid collected as outlined by Jellett et al. (1989).

PCR and DGGE

Extraction of the different sample types (healthy tissue, apparently healthy tissue, diseased tissue, swabs and coelomic fluid) were extracted using the Qiagen DNeasy blood and tissue kit. Bacterial 16S rRNA gene diversity was amplified using the primers 357-F (5'-CAG CAC GGG GGG CCT ACG GGA GGC AGC AG-3') and 518-R (5'-ATT ACC GCG GCT GCT GG-3'). Fungal diversity was assessed using a nested approach following the protocol laid out by Sweet et al. (2013). In brief, this consisted of an initial amplification using the primers ITS1-F (5'-CTTGGTCAT TTAGAGGAAAGTAA-3') and ITS4-R (5'-TCC TCC GCTTATTGATATGC-3') followed by a 1:100 dilution of the PCR product with the primers ITS3-F (5'-GCA TCG ATG AAG AAC GCAGC-3') and ITS4-R (5'-TCC TCC GCTTATTGATATGC-3'). Protozoan 18S rRNA gene diversity was amplified using the primers Cil-F (5'-TGG TAG TGT ATTGGACWA

CCA-3') and Cil-R (5'- TGA AAA CAT CCT TGG CAA CTG-3'). PCR protocols were the same as those outlined by Sweet & Bythell (2012) and Sweet et al. (2013). A GC clamp (CGCCCGCCGCGCCCGCG CCCGGCCCGCCGCCCCCGCCCC) was inserted onto the 5' end of the primers 357-F, ITS4-R and Cil-R, enabling use in denaturing gradient gel electrophoresis (DGGE). For each of the above primer pairs, we used 30 µl PCR mixtures containing 1.5 mM MgCl₂, 0.2 mM dNTP (Promega), 0.5 mM of each primer, 2.5 µl of *Taq* DNA polymerase (QBiogene), incubation buffer and 20 ng of template DNA (Sweet & Bythell 2012). DGGE was conducted using a 10% (w/v) polyacrylamide gel for bacterial 16S rRNA gene diversity and 8% (w/v) for fungal and protozoan diversity as in Sweet & Bythell (2012) and Sweet et al. (2013). Bands of interest (those which explained the greatest differences/similarities between samples) were excised from DGGE gels and re-amplified using the same PCR protocols as described above with the same original primers minus the additional GC clamps needed for DGGE analysis. These were then labelled using a Big Dye (Applied Biosystems) transformation sequence kit, and sent to Genevision (Newcastle University, UK) for sequencing.

454 pyrosequencing and analysis

After the initial results from DGGE analysis, 454 pyrosequencing was conducted for bacterial diversity only, using the same PCR primers as above, viz. 357-F (5'-CAG CAC GGG GGG CCT ACG GGA GGC AGC AG-3') and 518-R (5'-ATT ACC GCG GCT GCT GG-3'). PCR mixtures and conditions were the same as above with the following minor amendments: the primers used did not have the addition of the GC clamp, and HotStarTaq polymerase was used (Qiagen). PCR products for 454 pyrosequencing were then cleaned using AMPure magnetic beads (Beckman Coulter Genomics). Amplicon samples were then quantified using a Qubit fluorometer (Invitrogen) and pooled to an equimolar concentration. Sequences were run on 1/8 of a 454 FLX Titanium pico-titre plate at Newgene in the Centre for Life (Newcastle, UK).

Pyrosequences were processed using a QIIME pipeline (version 1.5.0) (Caporaso et al. 2010), using the SILVA reference database (release version SSU/LSU 123). Sequences were filtered and removed if they (1) were <50 nucleotides in length, (2) contained ambiguous bases (Ns) and/or (3) contained primer mismatches. Analysis using 2% single-linkage pre-

clustering and average-linkage clustering based on pairwise alignments was performed to remove sequencing-based errors. The remaining sequences were de-noised within QIIME. The resulting reads were checked for chimeras (using UCHIME) and clustered into >98% similarity operational taxonomic units (OTUs) using the USEARCH algorithm in QIIME. All singletons (reads found only once in the whole data set) were excluded from further analyses. After blast searches on GenBank, we retained the best BLAST outputs, i.e. the most complete identifications, and compiled an OTU table, including all identified OTUs and respective read abundances. In total, 748 892 raw nucleotide reads were produced with an average length of 49 bp, corresponding to 223.7 Mb. After filtering, a total of 492 540 quality reads were acquired. The length of the remaining sequences varied from 95 to 151 bp, with an average length of 121 bp. Technical control samples were processed in the same way as above, whereby samples consisting of just ethanol (used for preservation of the samples) were extracted and sequenced. No DNA was detected either after PCR or from the downstream processing.

An analysis of similarity (ANOSIM) was conducted to test differences in 16S rRNA gene bacterial assemblages as described by both the DGGE and 454 sequencing. In addition, similarity percentage (SIMPER) analysis was performed to determine which OTUs better explained differences and similarities between the sample types and replicates for both methods.

Culturing of the suspected pathogen and sequence/phylogenetic analysis

Crushed samples of freshly acquired healthy and diseased tissue were plated directly (100 µl) in triplicate serial dilutions (1:1, 1:10 and 1:100) on marine agar (1.8% marine broth [MB], Difco-2216 USA, 0.9% NaCl, 1.8% Agar Bacto, Difco-214010) and thio-sulphate citrate bile salts sucrose (TCBS) agar. Plates were incubated at 32°C for 24 h as in Séré et al. (2015). Cultivable bacterial strains exhibiting a unique colony were then routinely sub-cultured to purification under the same growth conditions for their subsequent use in inoculation experiments. Individual colonies were sequenced using the primer pair 27F (AGAGTTTGTATCMTGGCTCAG) and 1492R (GGTTACCTTGTTACGACTT) following the protocols outlined by Séré et al. (2015). Only certain bacteria identified as potential pathogens

from the previous DGGE and 454 pyrosequencing were specifically targeted, i.e. from the genus *Vibrio*. To confirm identification of the cultured vibrios, we compared the best match achieved from the 16S rRNA gene bacterial sequence to the best match achieved from the sequence of the housekeeping gene *pyrH*. The housekeeping gene was sequenced using the primers *pyrH*-F (ATGASNACBAAAYCCWAAACC) and *pyrH*-R (GTRAABGCNGMYARRTCCA) following the protocols outlined by Séré et al. (2015). The sequences obtained were aligned with reference sequences related to multiple bacterial strains selected from NCBI using the GENEIOUS alignment method. Additionally, sequences were concatenated and aligned against corresponding concatenated sequences (Thompson et al. 2005). Phylogenetic trees were built by the neighbour-joining method using the NKY model of GENEIOUS™ Pro (V.6.1.5) with bootstrap values based on 1000 replicates to further confirm identification of the pathogenic agent (see Fig. S3 in the Supplement, available at www.int-res.com/articles/suppl/m551p171_supp.pdf).

Association of potential pathogens with tissue damage

A further set of samples (n = 10 per sample type for each species) were collected as for microbial analysis. However, in this instance, samples were preserved with 5% paraformaldehyde for 24 h and then stored in 100% EtOH at 4°C. Half of these samples were embedded in LR white resin (Sigma-Aldrich) after dehydration steps consisting of 30 min intervals in 25, 35, 45, 55, 65 and 75% acetone with a final 2 steps in 100% acetone for 1 h each. These samples were used for immuno-histological light microscopy and transmission electron microscopy (TEM). Survey sections of 1 µm were cut and stained with the general stain 1% toluidine blue in 1% borax. For each tissue type, the locations of microorganisms were recorded using 0.01% acridine orange (Smith et al. 2014). The stain nigrosin (Smith et al. 2014) was also used for evaluating the extent of mass tissue necrosis. All sections were viewed under epifluorescence microscopy with an FITC-specific filter block (Nikon), and images were recorded using an integrated camera (Model JVC KY-SSSB: Foster Findlay and Associates).

For TEM, ultrathin sections (ca. 80 nm) were cut using a diamond knife on an RMC MT-XL ultramicrotome. These were then stretched with chloroform to eliminate compression, mounted on Pioloform-

filmed copper grids and stained with 2% aqueous uranyl acetate and lead citrate (Leica). The grids were examined using a Philips CM 100 Compustage (FEI) transmission electron microscope, and digital images were collected using an AMT CCD camera (Deben). Bacterial abundance was measured by sectioning samples ($n = 3$) of each tissue type of both urchin species and imaging on the TEM, with fields of view ($n = 20$) at a magnification of 2600 \times .

The remainder of the samples ($n = 5$ per tissue type for each species) were used for scanning electron microscopy (SEM). These were dehydrated in 25, 35, 45, 55, 65 and 75% ethanol (30 min at each interval), then a further 2 \times 1 h in 100% ethanol, with final dehydration using carbon dioxide in a Baltec critical point dryer. Specimens were then mounted on an aluminium stub with Acheson silver DAG, dried overnight and coated with gold (standard 15 nm) using a Polaron SEM coating unit. Specimens were examined using a Stereoscan 240 SEM, and digital images were collected by Orion 6.60.6 software.

Expt 1: transmission of lesions

A laboratory experiment was conducted to estimate the potential rate of transmission of the disease between individuals of *H. purpurascens* in the Australian winter (first trial; June 2012) and summer (second trial; January 2013). Individuals (25–40 mm) were collected from kelp (*Ecklonia radiata*) at Fairlight, immediately placed in aerated seawater and transported to Macquarie University. Separate collections were carried out for each trial. Experiments were run under 2 sets of temperature regimes, one representing present conditions in the field at the respective time of year (Manly hydraulics data), and a second set representing predicted future temperatures (a rise of 2°C) at the field site (the IS92 A2 scenario by the IPCC for 2060; Ridgway 2007). Therefore, temperatures used during the winter experiment were 19 and 21°C, and those used during the summer experiment were 21 and 23°C.

At the start of each trial, 8 urchins were added to 40 l aerated aquariums that had been randomly allocated a specific treatment (3 aquaria per treatment–health state combination); temperature treatments were ‘ambient’ and ‘predicted’ temperature, and health states were ‘no lesion’ and ‘lesion present’. The number of urchins used per aquarium was chosen to reflect the density range found naturally at the time of collection of individuals on *E. radiata* at Fairlight (Bell et al. 2014). ‘No lesion’ treatments con-

tained 8 *H. purpurascens* that appeared healthy and had no lesions at the start of the trial. ‘Lesion present’ treatments included 1 individual out of the 8 with a single small lesion, with the other 7 showing no signs of lesions. Urchins were fed ad libitum with *E. radiata*, their preferred food source (Williamson & Steinberg 2012). Water was changed approximately 3 to 4 times each week, and there was no exchange of water between tanks or treatments. Survivorship and the number of lesions on each individual were measured at the end of each week. Individuals developing lesions were left in the aquaria, but those that died were removed on a daily basis to avoid any perceivable effects of decay processes. Trials were terminated after 8 wk.

Expt 2: fulfilment of Henle–Koch postulates

For this part of the study, 16 apparently healthy urchins from both species (*H. erythrogramma* and *H. purpurascens*) were kept in individual tanks with the aim of avoiding any possible confounding effects due to inter-urchin interactions. The tanks were randomly assigned 1 of 5 treatments: control–no inoculation, control–inoculation (with the non-pathogenic bacterium *Marinobacter aquaeolei* [ATCC 700491]) or ‘low’, ‘medium’ or ‘high’ concentrations of the proposed pathogen, *Vibrio anguillarum* (see below). The non-pathogenic *M. aquaeolei* was used solely as a means of testing whether the inoculation procedure affected the urchins in any way and not as a means of testing virulence of the proposed pathogen. Colonies of *V. anguillarum* were cultured on vibrio-specific growth medium (TCBS agar) (Frans et al. 2011; see methodology in ‘Culturing of the suspected pathogen and sequence/phylogenetic analysis’ above). A single pure colony was then subsequently cultured in Marine Broth 2216 (Difco), then diluted to ‘low’, ‘medium’ and ‘high’ concentrations corresponding to 10², 10⁴ and 10⁶ colony-forming units (CFU) ml⁻¹ (Sweet et al. 2015). Such concentrations were determined from direct plate counts and comparison of culture turbidity with McFarland standards. Inoculation doses were tested in the 3 concentrations as above (cultured concentrations).

Free-flowing water was run through the tank systems during the entirety of the trial; however, during the inoculation process, the water flow was stopped, the appropriate inoculum of cells added to each treatment, and the aquaria were individually aerated for 5 h (Sweet et al. 2015). During this time, there was no detectable change in temperature of the aquarium

water (21°C), which was monitored using Hobo Data Loggers. After a 5 h exposure, the water flow was restarted. The trial was conducted over 14 d. Throughout the experimental process, visual observations of the contraction and/or extent of external lesions were recorded and compared to those occurring in the wild. At the end of the 14 d trial, $n = 8$ tissue samples were taken for both histology and microbial analysis in the same manner as that for the wild individuals (described above).

Estimation of R_0

The estimation of the reproduction number (R_0), i.e. the average number of secondary infections caused by 1 infected individual, is a critical component of understanding disease dynamics and making predictions in wild populations. It is usually assumed that a reproduction number greater than 1 indicates a high probability of an epidemic developing. However, such estimations of R_0 are often difficult to make as they are based on few data points. Furthermore, most methods of estimation require the generation time of the pathogen, the mean time lag between infection in a primary case and that in a secondary case (Obadia et al. 2012). Here, we did not have this information for the wild populations, so we used a simpler but less refined method, as outlined by Diekmann et al. (2013). This method is based on the estimation of the exponential growth rate, r . We assumed a closed population and a susceptible–infected–removed disease dynamic. Under these circumstances, if the incidence grows exponentially, R_0 is related to r in the following way, where γ is the mortality rate;

$$r = (R_0 - 1)\gamma \quad (1)$$

The minimum period between collections of diseased individuals in the field was approximately 1 yr and, given the rapid mortality of specimens in controlled aquaria experiments (see previous subsection), it is reasonable to assume a mortality rate of 1 between samples. Exponential growth of disease incidence can then be described by

$$\text{incidence}(t) = e^{rt} \quad (2)$$

where t is time, and incidence (t) is the incidence at time t . By taking the natural log of both sides of the equation, we can obtain the linear form

$$\ln[\text{incidence}(t)] = rt \quad (3)$$

Thus, r can be estimated using the beta coefficient (the slope) of a linear regression, with $\ln(\text{incidence})$

as the dependent variable and time as the independent variable. This value can then be substituted into Eq. (1) to estimate R_0 . R_0 is best estimated over the initial spread of the disease. We therefore calculated 2 estimates, one based on records up to and including 2005, and the second based on all records up to and including 2013, which allowed us to also examine the consistency of the estimation.

RESULTS AND DISCUSSION

Natural occurrence, transmission and spread of the disease

Two urchin species, *Heliocidaris erythrogramma* and *Holopneustes purpurascens*, are prominent grazers throughout shallow subtidal rocky reefs around south-eastern Australia (Wright et al. 2005). Although much is known of their ecology and biology (Williamson & Steinberg 2012, Keesing 2013), disease has not been identified as an issue for concern until this study. Diseased individuals of both species were first recorded during routine sampling in 1996. Inflicted urchins exhibited symptoms consisting of distinctive dark mucoid lesions on the epidermal tissue overlying the test and a loss of spines around the lesion (Fig. 1a,b). This pathology shares numerous similarities with the well documented diseases described for *Diadema antillarum* in the 1980s throughout the Caribbean and a more recent disease outbreak for *D. africanum* in the subtropical eastern Atlantic (Lessios et al. 1984, Lessios 1988, Clemente et al. 2014). Here we show that, from the first record of this disease, incidences of the number of individuals displaying lesions have increased, although the estimates of incidence have not always increased from year to year (Fig. 2). Furthermore, there is also a positive correlation between the number of diseased individuals observed and increases in the sea surface temperature (SST) within the region (Fig. 2), again a result reflective of many other diseases in the marine environment. In order to test whether there is indeed a relationship between increases in SST and disease occurrence (Fig. 2), a laboratory experiment was conducted to estimate the potential rate of transmission of the disease between individuals of one of the species, *H. purpurascens*, in both the Australian winter (first trial; June 2012) and summer (second trial; January 2013). Experiments were run under 2 sets of temperature regimes, one representing present conditions in the field at the respective time of year (Manly hydraulics data), and a second set represent-

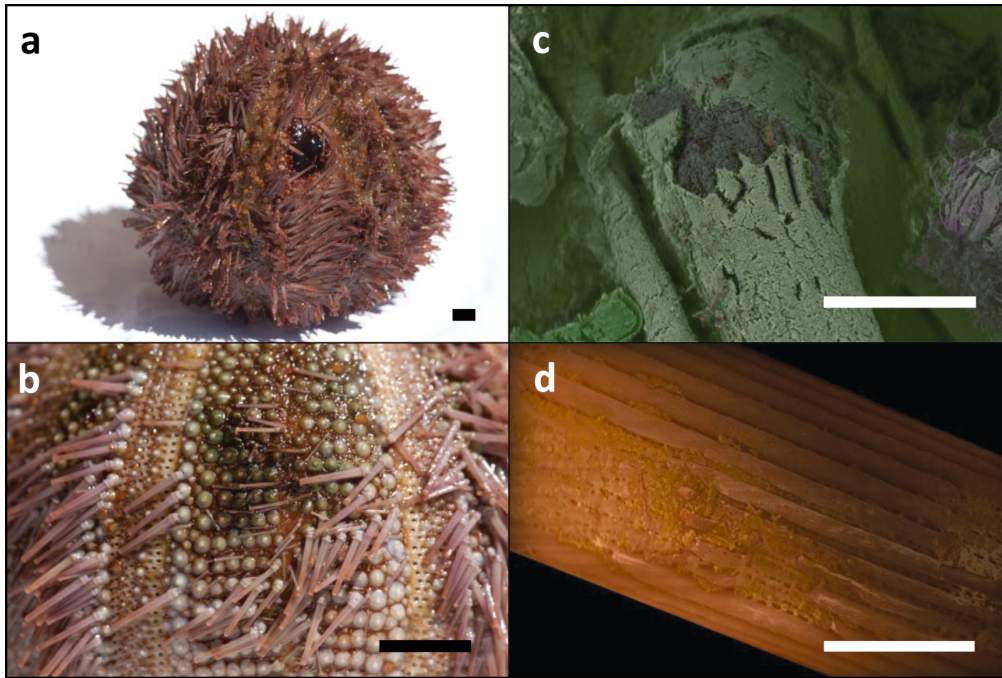


Fig. 1. *Holopneustes purpurascens*. (a) Diseased individual showing the characteristic dark mucoid lesions on the epidermal tissue overlying the test. (b) Loss of spines often occurs around the lesion and spreads outwards in a circular pattern. Photo by Paul Edward Duckett. (c,d) Scanning electron micrographs of diseased tissues, showing the effect on the surface of the spines; damage appears purplish (c) or yellowish (d). Scale bars = 5 mm (a and b) and 0.5 mm (c and d)

ing predicted future temperatures (a rise of 2°C) at the field site (the IS92 A2 scenario by the IPCC for 2060). In these experimental trials, all urchins that were exposed to individuals with lesions exhibited symptoms of the disease within an 8 wk period, regardless of the season (Fig. 3), highlighting that an increase in temperature is not required for individuals to contract the disease. However, symptom development (as indicated by the presence of lesions), was faster in treatments at elevated temperatures than in those at ambient temperatures (Fig. 3). In all instances, urchins that developed lesions either developed a greater number of lesions over time or died. It must be noted that 1 individual developed a lesion in the control tanks; however, this occurred in the summer during a period of elevated temperature (Fig. 3), and the individual was most likely infected in the wild but not identified as such before the experiment was initiated. Although the limitations of mesocosm experiments such as this one (Spivak et al. 2011) cannot be ignored, we believe that the results shown here highlight the importance of temperature as a driver of disease spread

and/or transmission, with a faster rate of transmission and earlier mortality being observed at higher temperatures (Fig. 3). Although we cannot say for sure that an increase in temperature in the environment has resulted in the observed increase in disease incidence, records do show that since the early 1990s,

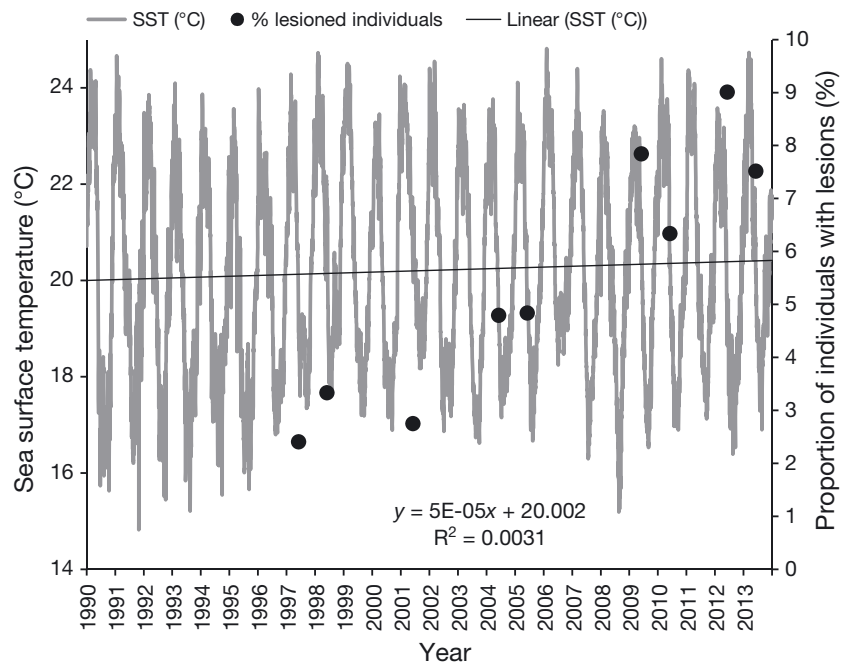


Fig. 2. Positive correlation between the proportion of *Holopneustes purpurascens* individuals with lesions and increased sea surface temperature

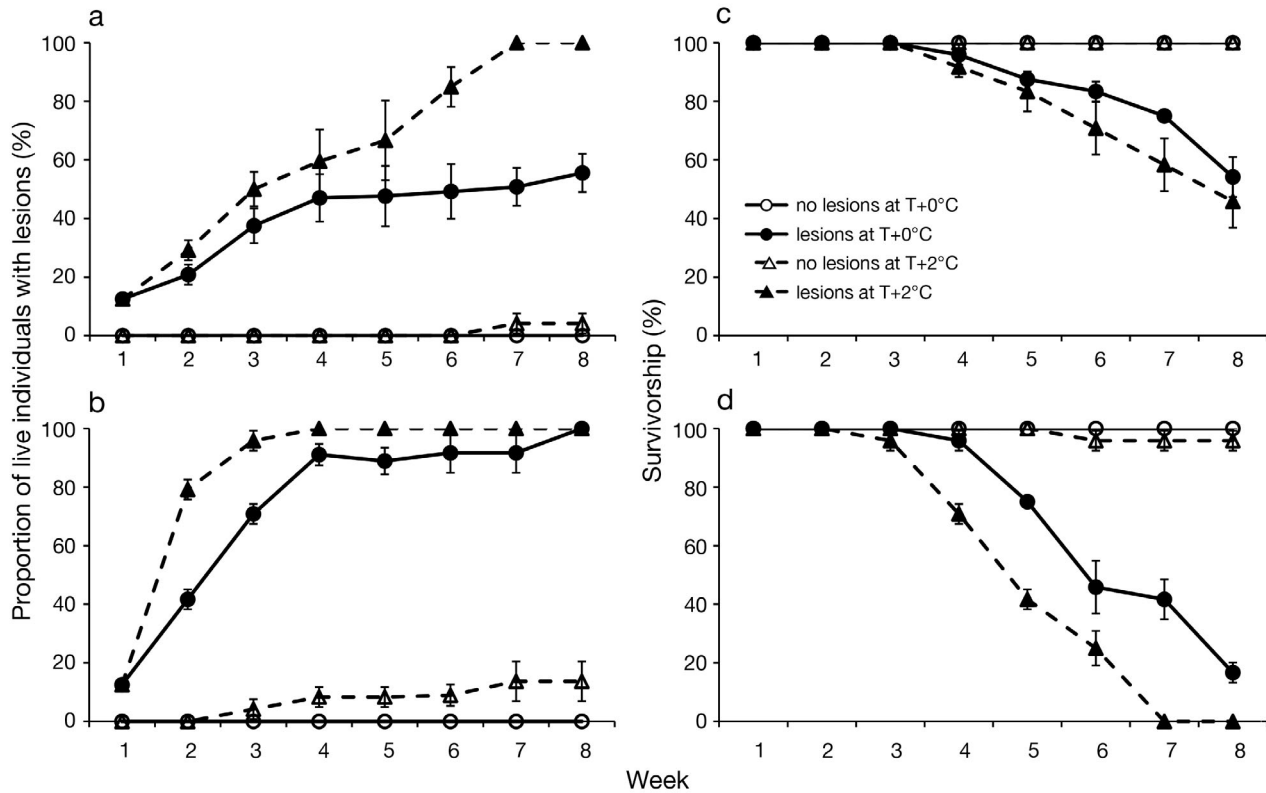


Fig. 3. Experimental trials with *Holopneustes purpurascens* (treatments: with or without lesions and with [+2°C] or without [+0°C] temperature [T] increase), illustrating contraction of the disease (i.e. occurrence of lesions) and survivorship. Proportion of live individuals with lesions over the 8 wk trial period for (a) winter and (b) summer, and survivorship over the same 8 wk period for (c) winter and (d) summer

SSTs, from satellites positioned over the sample site at Bare Island, have risen on average by 0.52°C to date (Fig. 2) (A. Wray-Barnes unpublished data). Furthermore, although the overall process of transmission in our study cannot be concluded from experiments such as those conducted here, we hypothesise that the causal agent in this study is waterborne, as lesions appeared to spread (during Expt 1) without contact being necessary. Again, such a result mirrors initial observations made during the 1980s *Diadema* die-off (Hunte et al. 1986, Clemente et al. 2014). However, to confirm this hypothesis, further tests of the surrounding water column, both in the field and in any further experimental trials, would be necessary. This would allow us to assign presence of the proposed pathogen within the environment.

Identification of potential pathogens associated with the disease

Both DGGE and 454 pyrosequencing using rDNA amplicons were used to assess the microbial communities associated with healthy urchins, and those

associated with diseased tissue, apparently healthy tissue (those associated with tissue on diseased individuals that still appeared healthy) and the coelomic fluid of both *H. erythrogramma* and *H. purpurascens* (see methodology in 'Identification of potential aetiological agents' above). This was conducted in order to assign potential microbial causal agents to this disease. No protozoans were detected in any of the tissues and/or the coelomic fluid, and only 1 fungal ribotype (a *Pleosporales* sp.) was detected on any of the urchin tissues, and this was consistently detected in all samples from both species. In contrast, a much greater diversity of bacterial OTUs were detected from all sample types. Furthermore, there were significant differences between the bacterial diversity of healthy, apparently healthy and diseased tissue for urchins from both species (*H. erythrogramma* and *H. purpurascens*; ANOSIM, $R = 1$, $p = 0.001$ and $R = 1$, $p = 0.002$ respectively—based on 454 pyrosequencing data). Both the DGGE profiles and 454 sequence analysis showed similar significant differences between groupings; however, we only report results from the 454 pyrosequencing hereafter. In total, 11 bacterial OTUs were detected on healthy individuals.

These were consistent between replicates of both species and are likely to be surface associated, as there were no significant differences between swab samples (i.e. surface-associated bacteria) and those of the 'complete' crushed tissue samples ($R = 0.97$, $p = 0.12$). From these 11 bacterial OTUs found on healthy, non-diseased individuals (see the heatmap in Table S1 for full details on NGS OTUs found between the samples), a *Mycobacterium*, a *Comamonadaceae* and a *Xanthomonadaceae* were detected in all replicates of the healthy tissue (non-diseased) samples and only in *H. purpurascens* (Table S1 in the Supplement). The bacterial communities associated with these 'apparently healthy' tissues (i.e. visibly healthy tissues on a diseased individual) showed an increase in bacterial diversity yet were more similar (between replicates) to those associated with healthy tissues than to diseased tissues, despite originating from an infected individual (Table S1). Differences were observed in the bacterial communities between apparently healthy tissues from the 2 urchin species, with *H. purpurascens* harbouring 31 individual OTUs compared to 25 in *H. erythrogramma*. Only 4 OTUs were found in the apparently healthy tissue and were absent in healthy tissues across both urchin species, including a *Micrococcaceae* sp., a *Tenacibaculum* sp., a *Kordiimonadaceae* sp. and a *Vibrio* sp. (Table S1). The diseased tissues harboured an even greater diversity of bacteria, with many bacterial OTUs present between both species (Table S1). However, only *Vibrio* was consistently detected in both diseased urchins and across all replicate samples, as might be expected of a causal agent. *Vibriosis* are routinely detected as aetiological agents and are ubiquitous in the marine environment (Morris & Acheson 2003). Indeed, a recent study by Clemente et al. (2014) highlighted that a potential causal agent for the recent mass mortality event effecting up to 65% of *D. africanum* is another member of this group, *V. alginolyticus* (Clemente et al. 2014).

Interestingly, we also detected bacteria present in the coelomic fluid of 2 of the diseased urchins sampled in this study. However, only 1 bacterial species was detected within these samples, i.e. the same *Vibrio* detected in the diseased tissues. These same samples showed a more advanced stage of the disease, evidenced by the histological sections (Fig. 4d,h). In all other samples tested, there were no other detectable microbes (bacteria, fungi or protozoans) within this area, leading us to suggest that in these individuals, a more advanced stage of the disease was present. In healthy urchins, the coelomic

fluid is usually a sterile environment (Kaneshiro & Karp 1980), maintained by both bactericidal properties of the coelomic fluid (Turton & Wardlaw 1987) and by coelomocytes that phagocytise foreign organisms and particles (Dybas & Fankboner 1986). This finding corresponds with previous studies which have found similar pathogenicity for 2 other urchin diseases, i.e. bald sea urchin disease (Maes & Jangoux 1984, 1985) and deep sea vibrio urchin disease (Bauer & Young 2000), where the coelomic fluid of these urchins was also infected by bacteria during disease outbreaks.

Association of potential pathogens with tissue damage

Histological sections of healthy urchin tissues showed clear organised structure, displaying healthy cells and muscle structure (Fig. 4a). Whilst most of the cells in the apparently healthy tissues were still comparable to those in healthy samples, some cells were showing the beginnings of a breakdown of the structure and appeared to be lysing (Fig. 4b). However, in contrast to the pathology reported for the *Diadema* disease in the Atlantic (Clemente et al. 2014), there was no visible sign of tissue necrosis (Fig. S2 in the Supplement). A few rod-shaped bacteria were detected in the apparently healthy tissue, but these occurred in relatively low numbers (2 ± 2 bacteria μm^{-2} of tissue, mean \pm SE, $n = 50$ sections) and were not consistent between replicates. In contrast, diseased tissues showed cells that were non-functional (lack of orange staining in histological samples), and the tissue structure showed evidence of extensive breakdown (Fig. 4c). During the latter stages of disease onset (Fig. 4d), the tissue structure had completely collapsed, with no organisation visible. In these samples, bacteria were present in significantly larger numbers (28 ± 16 bacteria μm^{-2} of tissue, mean \pm SE, $n = 50$ sections) and appeared deep within the tissue structure (Fig. 4c,d). Transmission electron micrographs elucidated how the structures of the tissues were affected by the bacterial pathogens with a clear distinct cell-free band surrounding each bacterium (Fig. 4g, and see Fig. S1b in the Supplement). Both muscle tissues and collagen fibres appeared to be affected by the bacterium (Fig. S1b), leading to the observed breakdown of the tissue present in the latter stages of the disease (Fig. 4d,h). Scanning electron micrographs of the diseased tissues (Fig. 1c,d) showed that the external structure of the spine was affected and that the spines appeared

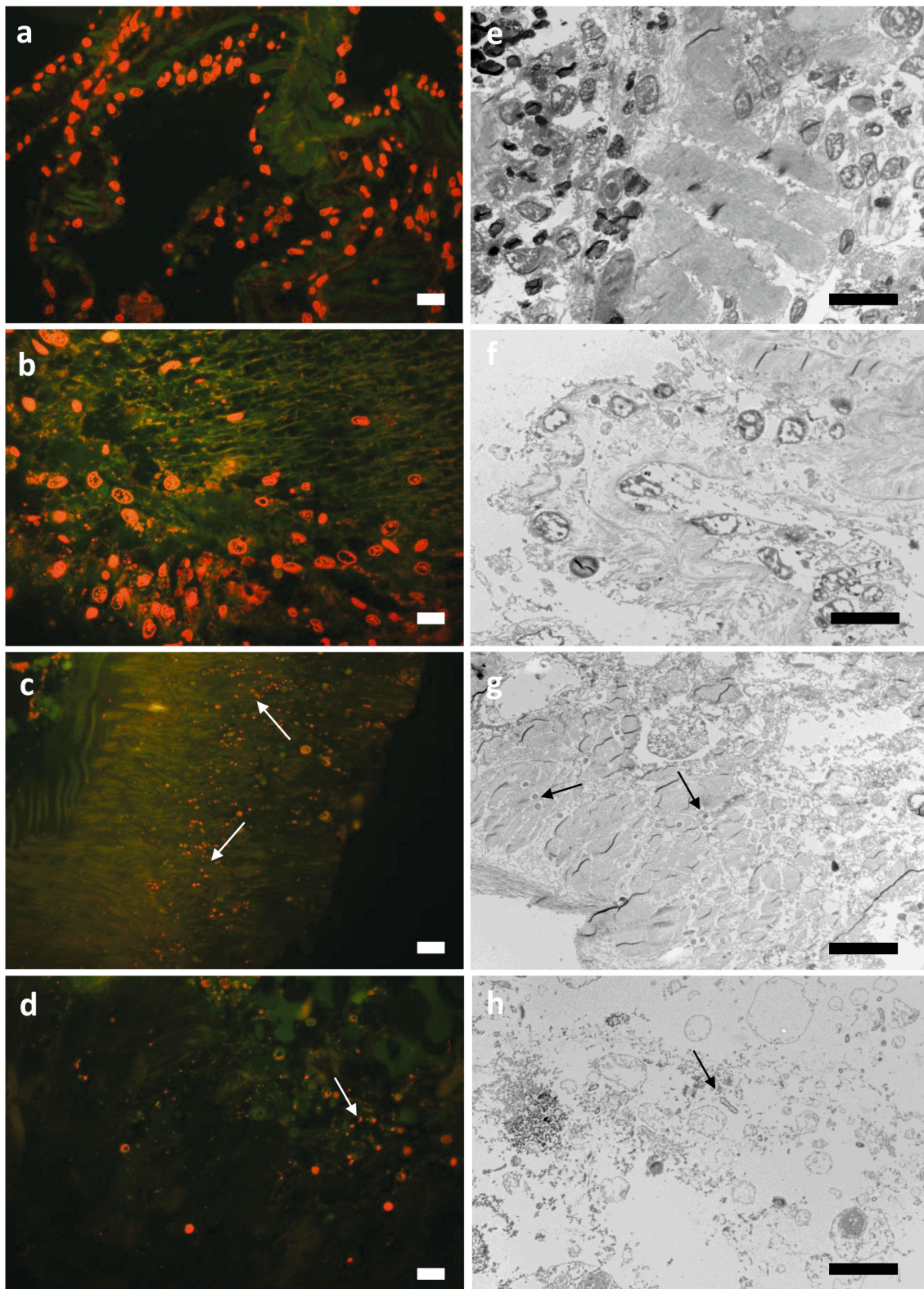


Fig. 4. Representative histological sections of healthy, apparently healthy and 2 different stages of diseased *Heliocidaris erythrogramma* tissues. (a,e) Healthy tissue, (b,f) apparently healthy tissue from a diseased individual, (c,g) early stage of disease taken at the disease lesion itself, (d,h) later stages of disease onset. Arrows highlight the presence of bacteria. Sections in panels a–d were stained with acridine orange; panels e–h show transmission electron micrographs. Scale bars = 10 μ m.

to collapse, giving rise to the characteristic visual lesions of the disease (a test devoid of spines) (Fig. 1a,b). Finally, no fungi, viruses or protozoa were identified within the tissues themselves, supporting the DGGE and 454 pyrosequencing mentioned above ('Identification of potential pathogens...').

Fulfilment of Henle–Koch postulates

The evidence from the bacterial profiling highlighted that a member of the genus *Vibrio* was the most likely pathogen responsible for this disease (see 'Identification of potential pathogens...' above). This *Vibrio* ribotype was absent in healthy tissues and present in all apparently healthy and diseased tissues sampled, from both species. Furthermore, vibrios were only able to be cultured from diseased tissue, adding further support to this theory. A subset of the cultured *Vibrio* colonies were sequenced, and all were identified (using both the 16S and *pyrH* house-keeping genes; see 'Materials and methods') as *V. anguillarum* (submitted to GenBank under accession no. KP001554). A pure culture of this bacterium was then used in the inoculation trials to fulfil Koch's postulates and confirm pathogenesis (Expt 2). Disease signs were induced in less than 48 h after inoculation. Upon the appearance of visual lesions (which were similar to those associated with the diseased individuals in the wild), all urchins ultimately succumbed within a further 76 h of contracting the disease. None of the uninoculated controls or those inoculated with the non-pathogenic bacterium died during the experiment, and none showed any visible signs of ill health. However, we cannot discount potential effects that the aquarium setup may have had on the urchins. It is therefore likely that the rate of death in the wild would be slower than that observed in these experiments, and further monitoring of diseased individuals *in situ* must be conducted. To fulfil the final steps of Koch's postulates, the same pathogen was re-isolated from experimentally diseased individuals and matched to the original inoculum (Hogue 1971). This evidence further supports the role of vibrios in this disease, in particular highlighting *V. anguillarum* as the likely causal agent in this study. This finding complements 2 previous studies (Gilles & Pearse 1986, Becker et al. 2007), which also showed that vibrios are responsible for diseases asso-

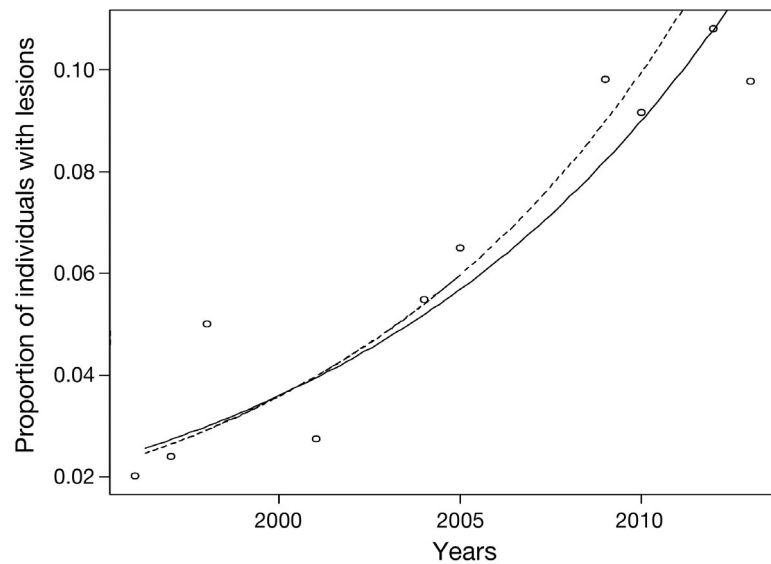


Fig. 5. Recorded disease incidence in *Holopneustes purpurascens* over time (circles). Curves represent the fitted exponential growth phase based on estimated intrinsic growth rates (r) from linear regression, using all records to 2013 (solid line) and records up to and including 2005 (dashed line)

ciated with 2 other urchin species, viz. *Strongylocentrotus purpuratus* (Gilles & Pearse 1986) and *Tripneustes gratilla* (Becker et al. 2007). Furthermore, the pathogenicity of *V. anguillarum* has been established for other marine organisms from a diverse range of taxa, including eels, oysters, fish and lobsters (Joseph et al. 2014, Tan et al. 2014, Wendling et al. 2014).

Modelling the current spread of the disease *in situ*

We also aimed to model the average number of secondary infections caused by any one infected individual at any given time *in situ* (also known as the reproduction number, R_0). Such information is a critical component to understanding disease dynamics in any system. $R_0 > 1$, for example, indicates a high probability of an epidemic developing. In this instance, the intrinsic rate of increase (r) was estimated at 0.0961 using the full temporal span of the incidence records (from 1996 to 2013), and 0.1019 using the data up to and including that for 2005 (see methodology in 'Estimation of R_d ', above). Incidence data and fitted exponential curves suggested values of R_0 as 1.096 (95% CI = ± 0.0139) and 1.10 (95% CI = ± 0.0405) (Fig. 5). This indicates a strong possibility that a disease epidemic may occur, or already has. Although we acknowledge that such estimates for epidemics should be treated with caution, namely as a number of assumptions have to be made during the

estimation process, our long-term sampling shows an increasing trend in disease incidence over the 17 yr period (although not always on a year to year basis), with an incidence of >0.1 recorded in 2012 (Fig. 5). Moreover, for this model, we also had to assume that the population was closed, which is actually conservative and probably unlikely, as both species are free spawners. Open populations promote re-infection of recovered patches from infected areas; therefore there is substantial potential for spatial dynamics to increase the likelihood of disease persistence over and above our current 'conservative' estimate.

To conclude, we have reported a disease of 2 common sea urchins in south-eastern Australia, and identified the causal agent as *V. anguillarum*. The symptomatology and transmission characteristics of this reported disease share similarities with the 2 *Diadema* die-offs in the Caribbean and the Atlantic, and 2 further diseases reported to affect another 2 urchin species, *S. purpuratus* and *T. gratilla*. Our results support the now widely accepted view that transmission of many diseases in the marine environment and virulence of specific pathogens such as those from the genus *Vibrio* increase at elevated temperatures (Vezzulli et al. 2010, Frans et al. 2011). Therefore, as with many other marine diseases associated with other marine taxa, this disease is likely to increase in severity and extent as SSTs rise as a result of climate change. Finally, we end with the suggestion that future studies should assess the pathogenicity of different isolated strains of *V. anguillarum*, as this was not tested in this current study and may have important implications regarding the spread of this disease.

Acknowledgements. Animals were collected under scientific collection permits from the Department of Primary Industries, New South Wales. We thank Alexander Wray-Barnes for use of his long-term dataset on SST. This research was partly funded by the Department of Biological Sciences at Macquarie University, and is contribution number 171 from the Sydney Institute of Marine Science.

LITERATURE CITED

- Ainsworth TD, Thurber RV, Gates RD (2010) The future of coral reefs: a microbial perspective. *Trends Ecol Evol* 25: 233–240
- Bauer JC, Young CM (2000) Epidermal lesions and mortality caused by vibriosis in deep-sea Bahamian echinoids: a laboratory study. *Dis Aquat Org* 39:193–199
- Becker P, Gillan DC, Eeckhaut I (2007) Microbiological study of the body wall lesions of the echinoid *Tripneustes gratilla*. *Dis Aquat Org* 77:73–82
- Bell JE, Bishop MJ, Taylor RB, Williamson JE (2014) Facilitation cascade maintains a kelp community. *Mar Ecol Prog Ser* 501:1–10
- Campbell AH, Vergés A, Steinberg PD (2014) Demographic consequences of disease in a habitat-forming seaweed and impacts on interactions between natural enemies. *Ecology* 95:142–152
- Caporaso JG, Kuczynski J, Stombaugh J, Bittinger K and others (2010) QIIME allows analysis of high-throughput community sequencing data. *Nat Methods* 7:335–336
- Carpenter RC (1986) Partitioning herbivory and its effects on coral reef algal communities. *Ecol Monogr* 56:345–363
- Clemente S, Lorenzo-Morales J, Mendoza JC, López C and others (2014) Sea urchin *Diadema africanum* mass mortality in the subtropical eastern Atlantic: role of waterborne bacteria in a warming ocean. *Mar Ecol Prog Ser* 506:1–14
- Diekmann O, Heesterbeek H, Britton T (2013) Mathematical tools for understanding infectious disease dynamics. Princeton Series in theoretical and computational biology. Princeton University Press, Princeton, NJ
- Dybas L, Fankboner PV (1986) Holothurian survival strategies: mechanisms for the maintenance of a bacteriostatic environment in the coelomic cavity of the sea cucumber, *Parastichopus californicus*. *Dev Comp Immunol* 10: 311–330
- Feehan CJ, Scheibling RE (2014) Effects of sea urchin disease on coastal marine ecosystems. *Mar Biol* 161: 1467–1485
- Frans I, Michiels CW, Bossier P, Willems KA, Lievens B, Rediers H (2011) *Vibrio anguillarum* as a fish pathogen: virulence factors, diagnosis and prevention. *J Fish Dis* 34:643–661
- Gilles KW, Pearse JS (1986) Disease in sea urchins *Strongylocentrotus purpuratus*: experimental infection and bacterial virulence. *Dis Aquat Org* 1:105–114
- Harvell CD, Kim K, Burkholder JM, Colwell RR and others (1999) Emerging marine diseases—climate links and anthropogenic factors. *Science* 285:1505–1510
- Hogue RS (1971) Demonstration of Koch's postulates. *Am Biol Teach* 33:174–175
- Hunte W, Côté I, Tomascik T (1986) On the dynamics of the mass mortality of *Diadema antillarum* in Barbados. *Coral Reefs* 4:135–139
- IPCC (Intergovernmental Panel on Climate Change) (2014) Climate change 2014: synthesis report. Contribution of Working Groups I, II and III to the Fifth Assessment Report of the Intergovernmental Panel on Climate Change. IPCC, Geneva
- Jellett JF, Wardlaw AC, Scheibling RE (1989) Experimental infection of the sea urchin (*Strongylocentrotus droebachiensis*) with a pathogenic amoeba (*Paramoeba invadens*): quantitative changes in the coelomic fluid in vivo and cellular interaction in vitro. *Dev Comp Immunol* 13:428–429
- Joseph FRS, Latha N, Ravichandran S, Devi ARS, Sivasubramanian K (2014) Shell disease in the freshwater crab, *Barytelphusa cunicularis*. *Int J Fish Aquat Stud* 1: 105–110
- Kaneshiro ES, Karp RD (1980) The ultrastructure of coelomocytes of the sea star *Dermasterias imbricata*. *Biol Bull (Woods Hole)* 159:295–310
- Keesing JK (2013) *Heliocidaris erythrogramma*. *Dev Aquacult Fish Sci* 38:369–379
- Lafferty KD (2004) Fishing for lobsters indirectly increases epidemics in sea urchins. *Ecol Appl* 14:1566–1573
- Lessios H (1988) Mass mortality of *Diadema antillarum* in

- the Caribbean: What have we learned? *Annu Rev Ecol Syst* 19:371–393
- Lessios HA, Cubit JD, Robertson DR, Shulman MJ, Parker MR, Garrity SD, Levings SC (1984) Mass mortality of *Diadema antillarum* on the Caribbean coast of Panama. *Coral Reefs* 3:173–182
 - Levitan DR, Edmunds PJ, Levitan KE (2014) What makes a species common? No evidence of density-dependent recruitment or mortality of the sea urchin *Diadema antillarum* after the 1983–1984 mass mortality. *Oecologia* 175:117–128
 - Maes P, Jangoux M (1984) The bald-sea-urchin disease: a biopathological approach. *Helgol Meeresunters* 37: 217–224
 - Maes P, Jangoux M (1985) The bald-sea-urchin disease: a bacterial infection. In: Keegan BF, O'Connor BDS (eds) *Proc 5th Int Echinoderm Conf, Galway, 24–29 September 1984*. AA Balkema, Rotterdam, p 313–314
 - Miskelly A (2002) *Sea urchins of Australia and the Indo-Pacific*. Capricornia Publications, Lindfield
 - Morris JG, Acheson D (2003) Cholera and other types of vibriosis: a story of human pandemics and oysters on the half shell. *Clin Infect Dis* 37:272–280
 - Mumby PJ, Hedley JD, Zychaluk K, Harborne AR, Blackwell PG (2006) Revisiting the catastrophic die-off of the urchin *Diadema antillarum* on Caribbean coral reefs: fresh insights on resilience from a simulation model. *Ecol Model* 196:131–148
 - Obadia T, Haneef R, Boëlle PY (2012) The R0 package: a toolbox to estimate reproduction numbers for epidemic outbreaks. *BMC Med Inf Decis Mak* 12:147
 - Pederson HG, Johnson CR (2007) Growth and age structure of sea urchins (*Helicidaris erythrogramma*) in complex barrens and native macroalgal beds in eastern Tasmania. *ICES J Mar Sci* 65:1–11
 - Ridgway KR (2007) Long-term trend and decadal variability of the southward penetration of the East Australian Current. *Geophys Res Lett* 34:L13613, doi:10.1029/2007GL 030393
 - Sammarco PW (1982) Echinoid grazing as a structuring force in coral communities: whole reef manipulations. *J Exp Mar Biol Ecol* 61:31–55
 - Scheibling RE, Hennigar AW (1997) Recurrent outbreaks of disease in sea urchins *Strongylocentrotus droebachiensis* in Nova Scotia: evidence for a link with large-scale meteorologic and oceanographic events. *Mar Ecol Prog Ser* 152:155–165
 - Séré MG, Tortosa P, Chabanet P, Quod JP, Sweet MJ, Schleyer MH (2015) Identification of a bacterial pathogen associated with *Porites* white patch syndrome in the Western Indian Ocean. *Mol Ecol* 24:4570–4581
 - Smith D, Leary P, Bendall M, Flach E, Jones R, Sweet M (2014) A novel investigation of a blister-like syndrome in aquarium *Echinopora lamellosa*. *PLoS One* 9:e97018
 - Spivak AC, Vanni MJ, Mette EM (2011) Moving on up: Can results from simple aquatic mesocosm experiments be applied across broad spatial scales? *Freshw Biol* 56: 279–291
 - Steinberg PD (1995) Interaction between the canopy dwelling echinoid *Holopneustes purpurascens* [sic] and its host kelp *Ecklonia radiata*. *Mar Ecol Prog Ser* 127: 169–181
 - Sweet M, Bythell J (2012) Ciliate and bacterial communities associated with white syndrome and brown band disease in reef building corals. *Environ Microbiol* 14:2184–2199
 - Sweet M, Burn D, Croquer A, Leary P (2013) Characterisation of the bacterial and fungal communities associated with different lesion sizes of dark spot syndrome occurring in the coral *Stephanocoenia intersepta*. *PLoS ONE* 8: e62580
 - Sweet M, Bulling M, Cerrano C (2015) A novel sponge disease caused by a consortium of micro-organisms. *Coral Reefs* 34:871–883
 - Tan D, Gram L, Middelboe M (2014) Vibriophages and their interactions with the fish pathogen *Vibrio anguillarum*. *Appl Environ Microbiol* 80:3128–3140
 - Thompson F, Gevers D, Thompson C, Dawyndt P and others (2005) Phylogeny and molecular identification of vibrios on the basis of multilocus sequence analysis. *Appl Environ Microbiol* 71:5107–5115
 - Turton GC, Wardlaw AC (1987) Pathogenicity of the marine yeasts *Metschnikowia zobelli* and *Rhodotorula rubra* for the sea urchin *Echinus esculentus*. *Aquaculture* 67: 199–202
 - Vezzulli L, Previati M, Pruzzo C, Marchese A, Bourne DG, Cerrano C, VibrioSea Consortium (2010) *Vibrio* infections triggering mass mortality events in a warming Mediterranean Sea. *Environ Microbiol* 12:2007–2019
 - Wendling CC, Batista FM, Wegner KM (2014) Persistence, seasonal dynamics and pathogenic potential of *Vibrio* communities from Pacific oyster hemolymph. *PLoS ONE* 9:e94256
 - Williamson J, Steinberg P (2002) Reproductive cycle of the sea urchin *Holopneustes purpurascens* (Temnopleuridae: Echinodermata). *Mar Biol* 140:519–532
 - Williamson JE, Steinberg PD (2012) Fitness benefits of size-dependent diet switching in a marine herbivore. *Mar Biol* 159:1001–1010
 - Williamson JE, Carson DG, de Nys R, Steinberg PD (2004) Demographic consequences of an ontogenetic shift by a sea urchin in response to host plant chemistry. *Ecology* 85:1355–1371
 - Wright JT, de Nys R, Steinberg PD (2000) Geographic variation in halogenated furanones from the red alga *Delisea pulchra* and associated herbivores and epiphytes. *Mar Ecol Prog Ser* 207:227–241
 - Wright JT, Dworjanyn SA, Rogers CN, Steinberg PD, Williamson JE, Poore AGB (2005) Density-dependent sea urchin grazing: differential removal of species, changes in community composition and alternative community states. *Mar Ecol Prog Ser* 298:143–156
 - Zeebe RE (2012) History of seawater carbonate chemistry, atmospheric CO₂, and ocean acidification. *Annu Rev Earth Planet Sci* 40:141–165